VOL. 6, NO. 12, DECEMBER 2011 ISSN 1819-6608
ARPN Journal of Engineering and Applied Sciences

www.arpnjournals.com

THE EFFECTS OF ASPECT RATIO ON HEAT TRANSFER ACROSS AIR LAYERS IN A SLOT-VENTILATED WALL CAVITY

Akin Odewole and Rodger Edwards
School of Mechanical, Aerospace and Civil Engineering, The University of Manchester, Manchester, United Kingdom
E-Mail: cardilac2005@yahoo.com

ABSTRACT

The effects of aspect ratio on heat transfer across air layers ($Pr \approx 0.71$) in a slot-ventilated wall cavity were numerically studied in this paper for Rayleigh number, Ra_w in the range of 1.4×10^5 to 12.0×10^5 using the Reynolds-Averaged Navier-Stokes (RANS) methodology. Large horizontal aspect ratios of 40 and 60 for the wall cavities investigated enable a two-dimensional approximation to be employed in the study of the heat transfer characteristics of the air layers over a range of temperature that is representative of extreme winter and summer conditions in the study. Using the RANS-based methodology, a small temperature difference between the front and back wall of the cavity reduces the cost of heating required for remediating moisture and condensation in the wall cavity during the winter in contrast to transferring a similar amount of energy using a large temperature difference. A maximum deviation of about 5.11% obtained between the Nusselt number of the cavity flow at a vertical aspect ratio, H/W of 40 and 60 shows that an increase in the vertical aspect ratio of the cavity does not significantly affect the heat transfer rate across the air layers.

Keywords: heat transfer rate, aspect ratio, moisture, condensation, Nusselt number, Rayleigh number.

1. INTRODUCTION

The study of natural convection in cavities is of great engineering importance since it finds applications in electronic equipment and packaging [1], crystal growth and solidification processes [2], hot or cold liquid storage systems [3], buildings (greenhouse ventilation, room ventilation, glazed windows, uninsulated walls and attics) [4], airflow in heat transfer equipment and in countless other configurations [5]. The nature of airflow within some of these enclosures may be of special interest in the regulation of air quality and homogeneity of parameters such as temperature, humidity and concentration of pollutants while it is used in the regulation of heat transfer rates between surfaces in other applications.

For a differentially heated cavity, the cavity fluid flows upward along the heated wall and then sinks along the cold wall. It was shown that in a thin slot-ventilated wall cavity, a maximum velocity of about 6m/s was obtained for ambient temperature ranging from -20 to 20°C against a fixed back wall temperature of 10°C required for the remediation of moisture and condensation in an uninsulated wall cavity in contrast to a maximum velocity of about 1.5m/s under the pressure-driven and the combined flow modes [6]. The characteristics of the velocity field in the above study therefore stimulate our interest to have an understanding of the effect of cavity aspect ratio on heat transfer across air layers for comfort conditioning during the summer and winter periods for residential buildings employing the cavity-wall construction approach investigated in [6]. The remaining sections of this paper are structured as follows: the methodology employed in this study is presented in section 2 while the results of the study are discussed in section 3 of this article, with suitable conclusions on this study presented in section 4 of this article.

2. METHODOLOGY

The wall cavity shown in Figure-1 below and investigated in [6] is employed for this study. However in this study, ambient temperature in the range -40 to 30°C is investigated to represent a wider extreme condition of winter and summer temperatures in contrast to a range of -20 to 20°C investigated in [6]. Detailed information about the computational model shown in Figure-1 under modeling conditions other than the one adopted in this paper can be obtained from [6].

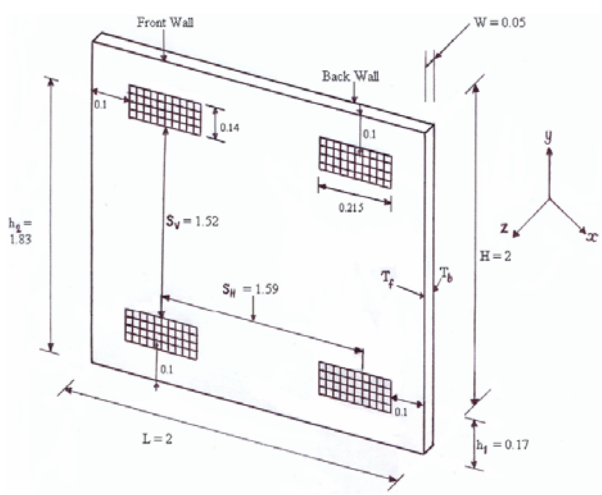

Figure-1. Configuration and dimensions (not drawn to scale) of the wall cavity, showing the ventilation slots. Square grids on the slots represent the ventilation baffles on these slots. All dimensions are in metres [6].

In order to model heat transfer in the wall cavity, a two-dimensional approximation, with the dimensions and configuration of the cavity shown in Figure-2 below, is employed for this study for an asymptotically large

VOL. 6, NO. 12, DECEMBER 2011 ISSN 1819-6608
ARPN Journal of Engineering and Applied Sciences

horizontal aspect ratio [7, 8]. A horizontal aspect ratio, L/W of 40 or 60 employed in this study thus not therefore appreciably affects the heat transfer results undertaken in the study.

In Figure-2, layers of air are enclosed between the vertical and end walls of the cavity. The vertical walls are isothermal plates of different temperature T_f and T_b, respectively for the front and back wall of the cavity while the end (upper and lower) walls of the cavity, representing limiting cases, are treated as adiabatic, that is zero heat flux (ZHF) between the walls and the air layers. To understand the effects of a change in the aspect ratio of the cavity on the characteristics of heat transfer across the air layers; the height, H (and width, L) of the cavity studied in Figure-1 is increased to 3m in Figure-2, with the 2 and 3m height of the wall cavity investigated in this paper.

The small size of the wall cavity studied in this paper enables a uniform mesh density with control volumes of 100,000 cells to be employed for the cavity with a vertical aspect ratio of 40 while control volumes of 150,000 cells are employed for the cavity with a vertical aspect ratio of 60. The size of the control volumes in each of these cases thus assists in employing an enhanced wall treatment approach in the discretization of the computational domains of the wall cavities. Using this wall treatment, a dimensionless wall distance y^+ of 1.60 obtained in each computational domain gives fine meshes sufficient enough to resolve the thickness of the laminar sub-layer [9].

For a fixed back wall temperature, T_b of 10^oC and varying ambient temperature, T_o of -40 to 30^oC employed in this study, the boundary conditions given in Equations (1) to (3) are prescribed on the walls of the cavity. The temperature of the cavity's front wall, T_f is assumed to be the same as that of the ambient, T_o. The cavity flow in this study is two-dimensional and incompressible, with the equations governing the cavity flow formulated using the Boussinesq approximation as shown in Equations (4) - (7) where the velocity components in the x- and y- directions respectively are u and v, T is the temperature, ρ is the cavity fluid's density, ν and α are the kinematic viscosity and thermal diffusivity of the cavity fluid respectively, g is the acceleration due to gravity and β is the coefficient of thermal expansion.

Equations (4) - (7) are solved using a pressure solver based on the Fluent codes [9] employing the second-order accurate central-differencing scheme for the diffusion terms, second order upwind scheme for the convection terms, PRESTO! Scheme for computing the pressure at the faces of control volumes while the SIMPLE algorithm was employed for coupling the pressure and the velocity terms of Equations (4) - (6) [10-12].

The incompressible laminar flow in the wall cavity studied was checked by ensuring that scaled residuals were less than 10^{-6} for all variables. The study of the thermal behaviour of the air layers enclosed in the wall cavity shown in Figure-2 is therefore carried out for Rayleigh number, Ra_W in the range of 1.4×10^5 to 12.0×10^5 while there is no significant variation in the Prandtl number, Pr (Pr varies from 0.71 to 0.72) of the air layers in the wall cavity.

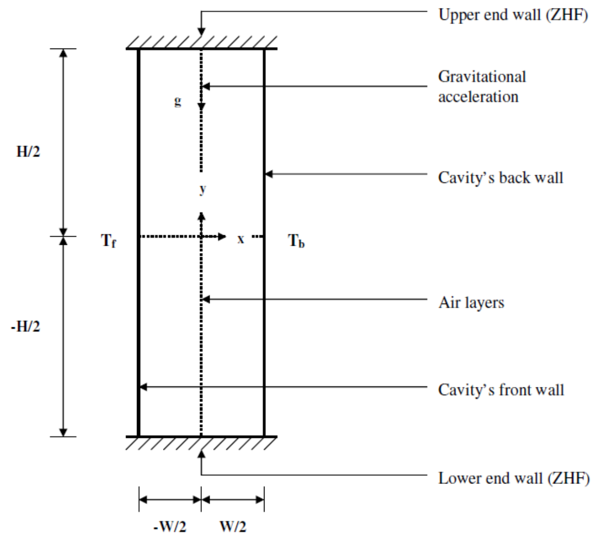

Figure-2. Schematic of the computational domain.

$$T = T_f \text{ at } x = -W/2 \tag{1}$$

$$T = T_b \text{ at } x = W/2 \tag{2}$$

$$\frac{\partial T}{\partial y} = 0 \text{ at } y = -H/2 \text{ and } y = H/2 \tag{3}$$

$$\frac{\partial u}{\partial x} + \frac{\partial v}{\partial y} = 0 \tag{4}$$

$$u\frac{\partial u}{\partial x} + v\frac{\partial u}{\partial y} = -\frac{1}{\rho}\frac{\partial p}{\partial x} + \nu\left(\frac{\partial^2 u}{\partial x^2} + \frac{\partial^2 u}{\partial y^2}\right) \tag{5}$$

$$u\frac{\partial v}{\partial x} + v\frac{\partial v}{\partial y} = -\frac{1}{\rho}\frac{\partial p}{\partial y} + \nu\left(\frac{\partial^2 v}{\partial x^2} + \frac{\partial^2 v}{\partial y^2}\right) + g\beta\left(T - T_{ref}\right) \tag{6}$$

$$u\frac{\partial T}{\partial x} + v\frac{\partial T}{\partial y} = \alpha\left(\frac{\partial^2 T}{\partial x^2} + \frac{\partial^2 T}{\partial y^2}\right) \tag{7}$$

3. RESULTS AND DISCUSSIONS

The temperature distributions, showing the transfer of heat across the air layers in the wall cavities investigated in this paper, are shown in Figures 3-6 below. Figures 3 and 4 show a two-dimensional wall cavity with a vertical aspect ratio, H/W of 40 while Figures 5 and 6 show a two-dimensional wall cavity with a vertical aspect ratio, H/W of 60. The temperatures of the air layers in the wall cavities are non-dimensionalised as shown in Equation (8) where a positive value is assumed for the reference temperature difference, ΔT ($\Delta T = T_b - T_f$) while the distance x is non-dimensionalised using the length W of the wall cavity.

VOL. 6, NO. 12, DECEMBER 2011 ISSN 1819-6608
ARPN Journal of Engineering and Applied Sciences

www.arpnjournals.com

$$\frac{T-T_c}{\Delta T} \tag{8}$$

The distributions of temperature shown by Figure-3 below indicate that heat is transferred by convection across a large fraction of the air layers in the wall cavity. This is indicated by the almost-zero gradient ($\partial T/\partial x \approx 0$) of the temperature profiles covering the range x/W = -0.5 to 0.5 while in the vicinity of the cavity walls, the transfer of heat is by conduction. Similar patterns of heat flow found in Figure-3 also occur in Figure-4. In the temperature distributions shown in Figure-4, however, there is a decrease in the size of air layers across which the transfer of heat is by convection. This phenomenon occurs at front wall temperatures greater than the back wall temperature, T_b. The numerical results shown in Figures 3 and 4 show large variations in heat transfer in the middle of the cavity and in the vicinity of the end walls.

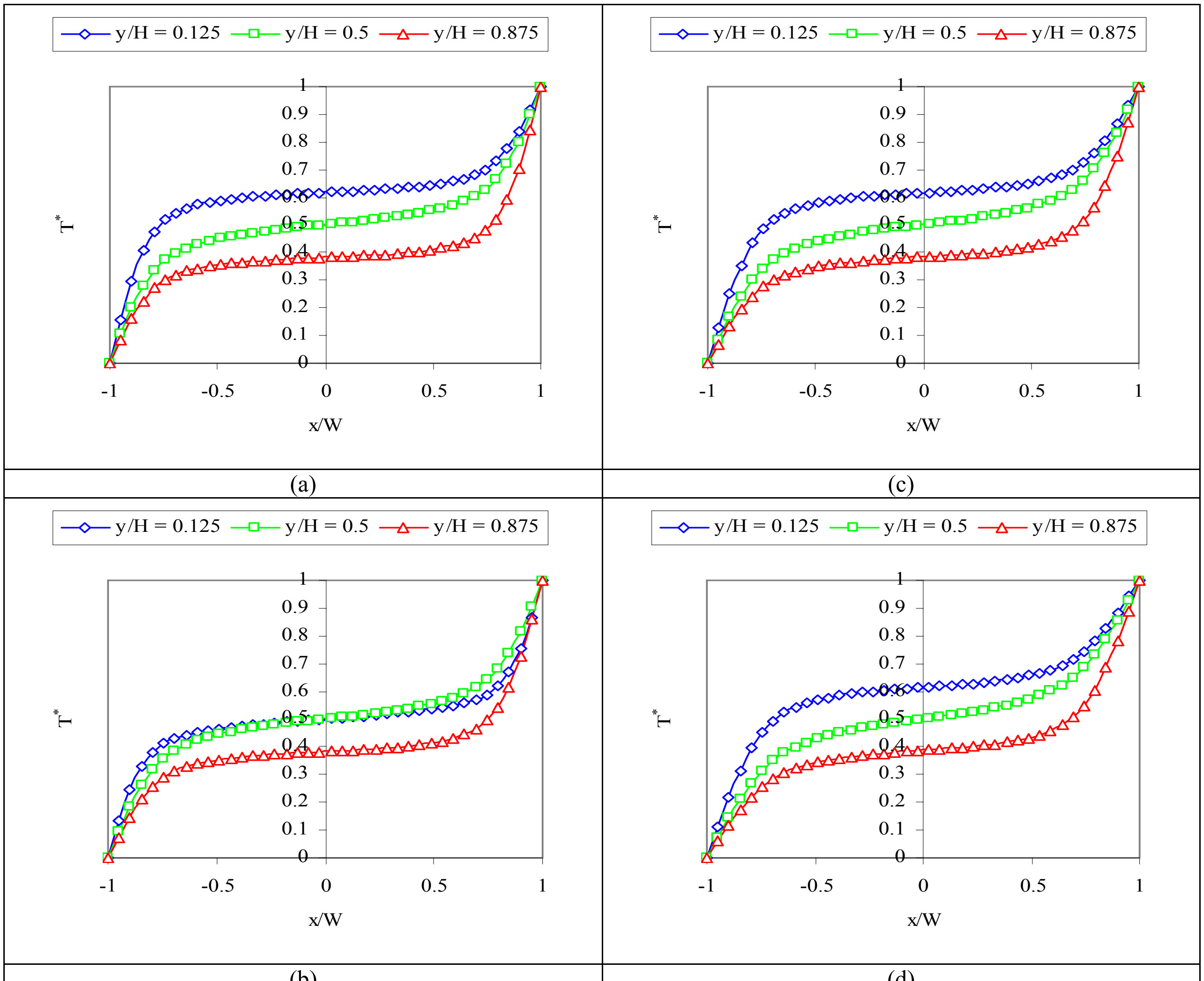

Figure-3. Horizontal temperature profiles in wall cavity for H/W = 40 and T_b = 283.15K: (a) T_f = 233.15K (b) T_f = 243.15K (c) T_f = 253.15K (d) T_f = 263.15K.

 ISSN 1819-6608
ARPN Journal of Engineering and Applied Sciences

www.arpnjournals.com

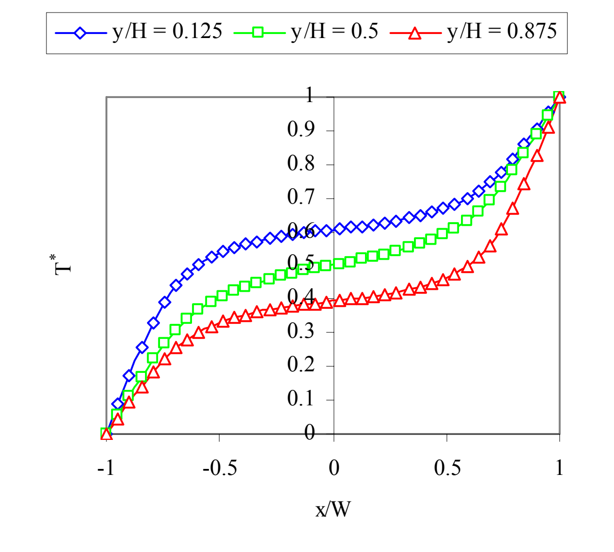

(a)

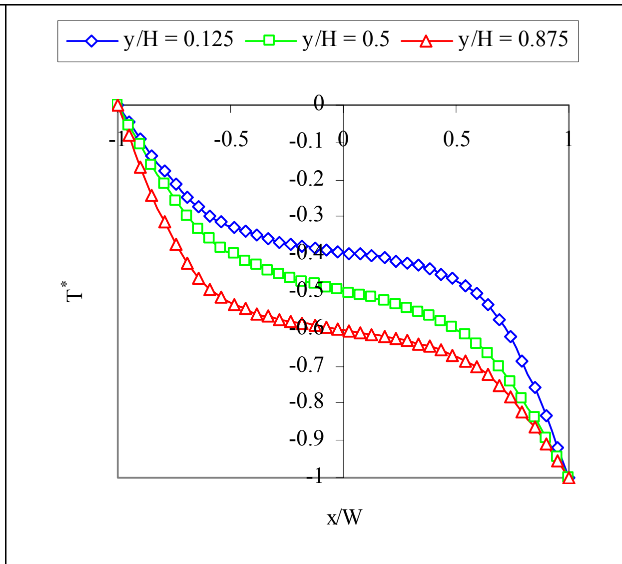

(b)

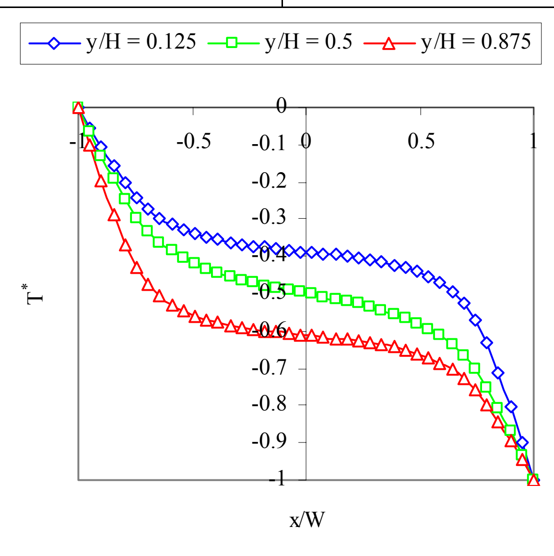

(c)

Figure-4. Horizontal temperature profiles in wall cavity for H/W = 40 and T_b = 283.15K: (a) T_f = 273.15K (b) T_f = 293.15K (c) T_f = 303.15K.

By increasing the vertical aspect ratio of the wall cavity from 40 to 60, the temperature distributions shown in Figures 5 and 6 are very close, indicating no significant difference in the heat transfer rate between the back and front wall of the cavity, as the cavity aspect ratio increases. An important feature of the numerical results shown in Figure-6 is that heat transfer by conduction occurs only in the thin layers of air (between x/W = -0.7 to -1 and 0.7 to 1) very close to the vertical walls of the cavity for a vertical aspect ratio of 60. The numerical results shown in Figures 5 and 6 at H/W = 60 are therefore insensitive to large temperature difference between the front and back wall of the cavity. The direction of heat flow under the temperature conditions in Figures 5 and 6 will therefore depend on whether or not T_f is greater than T_b. Under these conditions, the remediation of moisture and condensation in the wall cavity can be achieved by employing a small difference in temperature between T_f and T_b in the winter. This will ensure that the cost of heating is considerably reduced in contrast to using a large temperature difference between T_f and T_b to achieve a similar result in the winter. However during the summer when the temperature of the ambient is expected to increase, no heating may be required for the remediation of moisture and condensation in the wall

VOL. 6, NO. 12, DECEMBER 2011 ISSN 1819-6608
ARPN Journal of Engineering and Applied Sciences

www.arpnjournals.com

cavity. Under the condition of higher average ambient temperatures that characterise the summer period, the moisture content of the ambient air is lower and thus reducing the risk of moisture-laden air condensing on the walls of the cavity.

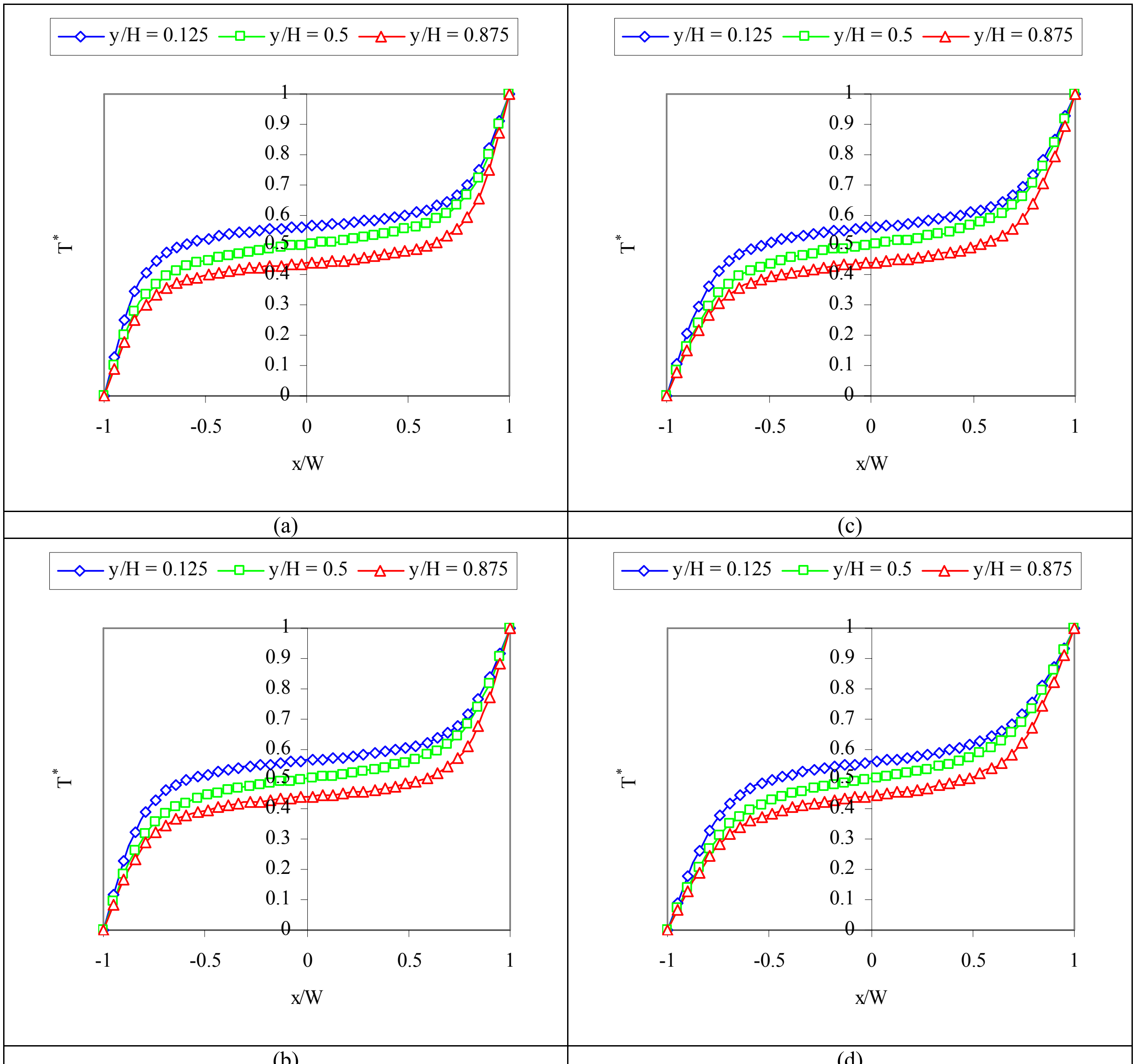

Figure-5. Horizontal temperature profiles in wall cavity for H/W = 60 and T_b = 283.15K: (a) T_f = 233.15K (b) T_f = 243.15K (c) T_f = 253.15K (d) T_f = 263.15K.

VOL. 6, NO. 12, DECEMBER 2011 ISSN 1819-6608
ARPN Journal of Engineering and Applied Sciences

www.arpnjournals.com

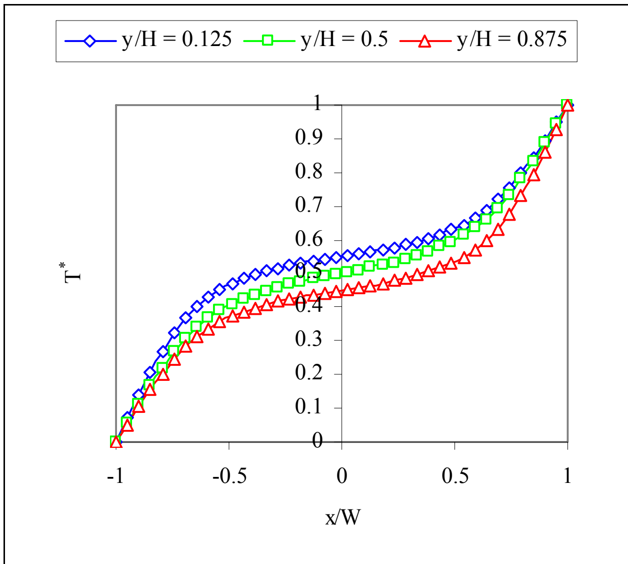

(a)

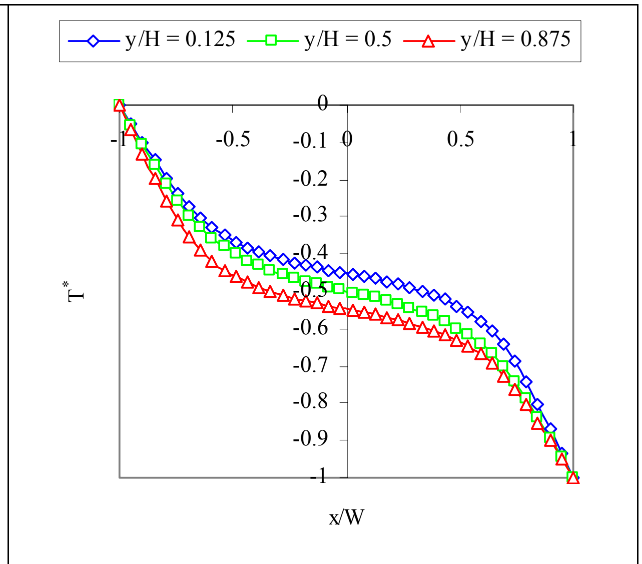

(b)

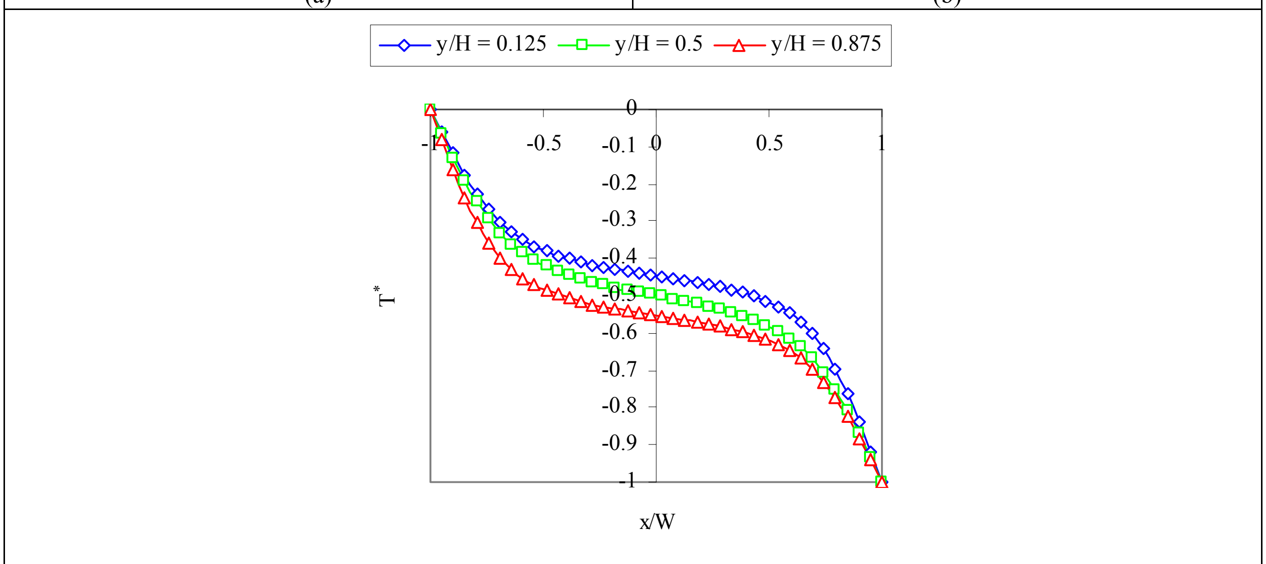

(c)

Figure-6. Horizontal temperature profiles in wall cavity for H/W = 60 and T_b = 283.15K: (a) T_f = 273.15K (b) T_f = 293.15K (c) T_f = 303.15K.

In order to understand the heat transfer characteristics of the cavity flow under the two vertical aspect ratios (H/W = 40 and 60) investigated in this study, the variation of the Nusselt number of the flow with varying Rayleigh number is presented in Figure-7 below. The Nusselt number of the air layers in the wall cavity decreases uniformly at lower Rayleigh numbers till about Ra = 1.7x105 is reached. Thereafter, a steady increase in the Nusselt number of the cavity flow is obtained as the Rayleigh number of the flow increases. The numerical results shown in Figure-7 indicates no significant difference in the Nusselt number of the cavity flow between H/W = 40 and H/W = 60, with a maximum deviation of 5.11% (shown in Table-1) obtained in the Nusselt number of the cavity flow when H/W is increased from 40 to 60. The numerical results shown in Figure-7 and Table-1 thereby also support the insensitivity of the cavity flow to large temperature difference between the front and back wall of the cavity.

VOL. 6, NO. 12, DECEMBER 2011 ISSN 1819-6608
ARPN Journal of Engineering and Applied Sciences

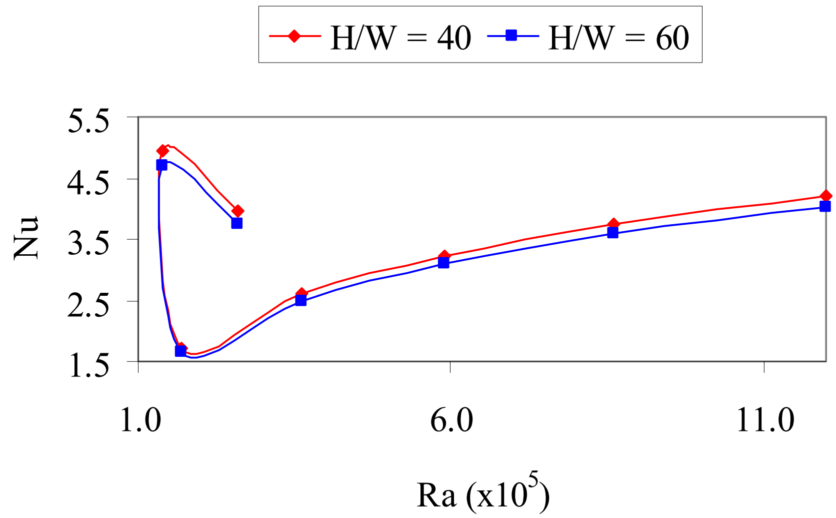

Figure-7. Nusselt-number variation of the cavity flow for varying Rayleigh number.

Table-1. Nusselt number values for different vertical aspect ratio.

H/W	Ra_w	Nu	H/W	Ra_w	Nu	**% Deviation**
40	$1.2x10^6$	4.211	60	$1.2x10^6$	4.033	4.23
	$8.6x10^5$	3.754		$8.6x10^5$	3.589	4.40
	$5.9x10^5$	3.234		$5.9x10^5$	3.086	4.58
	$3.6x10^5$	2.609		$3.6x10^5$	2.484	4.79
	$1.7x10^5$	1.728		$1.7x10^5$	1.641	5.03
	$1.4x10^5$	4.950		$1.4x10^5$	4.697	5.11
	$2.6x10^5$	3.952		$2.6x10^5$	3.757	4.93

4. CONCLUSIONS

In this study, the heat-transfer characteristics of air layers in a slot-ventilated wall cavity were investigated for a range of temperature that is representative of extreme thermal conditions in the winter and summer periods. The numerical results presented in this paper indicate that a small difference in temperature between T_f and T_b is required in the winter to transfer an approximately the same amount of energy between the front and back wall of an uninsulated cavity in a building in contrast to a large temperature difference between T_f and T_b. This reduces the cost of heating for remediating moisture and condensation in such a wall cavity in the winter. The numerical results also show that an increase in the vertical aspect ratio of the wall cavity from H/W = 40 to H/W = 60 does not significantly affects the rate of heat transfer between the air layers in the wall cavity. This is indicated by a maximum deviation of about 5.11% between the Nusselt numbers at H/W = 40 and those at H/W = 60. Whilst this may be due to the small depth (W = 50mm) of the cavities studied, future studies may include the effects of increasing depth of the cavity (W >50mm) on the heat-transfer characteristics of the air layers in the wall cavity.

REFERENCES

[1] Rodgers P. and Eveloy V. 2004. Application of low-Reynolds number turbulent flow models to the prediction of electronic component heat transfer. In: The 9th Intersociety Conference on Thermal and Thermomechanical Phenomena in Electronic Systems (ITHERM '04). 1: 495-503, June.

[2] Lartigue B., Lorente S. and Bourret B. 2000. Multicellular natural convection in a high aspect ratio cavity: experimental and numerical results. Int. J. Heat Mass Trans. 43: 3157-3170.

[3] Ramanan N. and Korpela S.A. 1989. Multigrid solution of natural convection in a vertical slot. Numerical Heat Transfer, Part A: Applications. 15(3): 323-339.

[4] Raithby G. D. and Wong H. H. 1981. Heat transfer by natural vertical air layers. Numerical Heat Transfer, Part A: Applications. 4(4): 447-457.

[5] Baelmans M., Meyers J. and Nevelsteen K. 2003. Flow modelling in air-cooled electronic enclosures. In: Proc. 19th Annual IEEE Semiconductor Thermal Measurement and Management Symp. (SEMI-THERM XIX). pp. 27-34, March.

[6] Odewole A. and Edwards R. 2011.The characteristics of the velocity field in a slot-ventilated wall cavity. ARPN Journal of Engineering and Applied Sciences. 6(10): 47-55.

[7] ElSherbiny S.M., Raithby G.D. and Hollands K.G.T. 1982. Heat transfer by natural convection across vertical and inclined air layers. J. Heat Transfer. 104: 96-102.

[8] Korpela S.A., Lee Y. and Drummond J.E. 1982. Heat transfer through a double pane window. J. Heat Transfer. 104: 539-544.

[9] Fluent 6.3 User's Guide. 2006. Fluent Inc., 10 Cavendish Court, Lebanon, NH 03766, USA.

[10] Ravi M.R., Henkes R.A.W.M. and Hoogendoorn C.J. 1994. On the high-Rayleigh-number structure of steady laminar natural-convection flow in a square enclosure. J. Fluid Mech. 262: 325-351.

[11] Moureh J. and Flick D. 2005. Airflow characteristics within a slot-ventilated enclosure. Int. J. Heat and Fluid Flow. 26: 12-24.

[12] Moureh J., Tapsoba M. and Flick D. 2009. Airflow in a slot-ventilated enclosure partially filled with porous boxes: Part I - Measurements and simulations in the clear region. Computers and Fluids. 38: 194-205.